4. Marchioli R, Finazzi G, Landolfi R, et al. Vascular and neoplastic risk in a large cohort of patients with polycythemia vera. *J Clin Oncol.* 2005;23(10):2224-2232. 10.1200/JCO.2005.07.062.

5. Vardiman JW, Thiele J, Arber DA, et al. The 2008 revision of the World Health Organization (WHO) classification of myeloid neoplasms and acute leukemia: rationale and important changes. *Blood.* 2009;114(5):937-951. 10.1182/blood-2009-03-209262.

6. Sørensen HT, Horvath-Puho E, Søgaard KK, et al. Arterial cardiovascular events, statins, low-dose aspirin and subsequent risk of venous thromboembolism: a population-based case-control study. *J Thromb Haemost.* 2009;7(4):521-528.

7. Berk PD, Wasserman LR, Fruchtman SM, Goldberg JD. Treatment of polycythemia vera: A summary of clinical trials conducted by the polycythemia vera study group. In: Wasserman LR, Berk PD, Berlin NI, eds. *Polycythemia Vera and the Myeloproliferative Disorders.* Philadelphia, PA: W.B. Saunders; 1995:166-194.

To the editor:

Cryptic *XPO1-MLLT10* translocation is associated with *HOXA* locus deregulation in T-ALL

Biological subclasses of T-cell acute lymphoblastic leukemia (T-ALL) can be defined by recurrent gene expression patterns, which typically segregate with specific chromosomal anomalies. The HOXA$^+$ subgroup is characterized by deregulated homeobox A (*HOXA*) gene expression and is associated with translocations involving the mixed lineage leukemia (*MLL*) and/or *MLLT10* loci, *SET-NUP214*, or *TCRB-HOXA*.[1,2] Nevertheless, the genetic basis for many HOXA$^+$ cases remains unexplained.

Diagnostic assessment of a 33-year-old man with T-ALL revealed high leukemic blast expression of *HOXA9* at levels comparable to those in known HOXA$^+$ cases (Figure 1A). Tests for *PICALM-MLLT10*, *SET-NUP214*, *MLL-AF6*, and *TCRB-HOXA* were negative. Leukemic cells exhibited a complex karyotype (46,XY,add(2)(p14),-10,-17,+2mars,inc[11]), which led us to speculate that HOXA positivity might be caused by a structural genetic abnormality. We therefore performed poly(A)-enriched sequencing (RNA-sequencing) of diagnostic RNA, analysis of which revealed fusion of exon 24 of *XPO1* to exon 6 of *MLLT10* (Figure 1B, upper panel). Expression of an in-frame *XPO1-MLLT10* fusion transcript was confirmed by reverse transcriptase polymerase chain reaction (RT-PCR) and direct sequencing (Figure 1B, lower panel).

We hypothesized that the common involvement of *MLLT10* would result in similar deregulation of *HOXA* locus expression in *XPO1-MLLT10*$^+$ and *PICALM-MLLT10*$^+$ T-ALL. We tested the expression of a range of *HOX* genes by quantitative RT-PCR. As predicted, the pattern of *HOXA* gene transcription in the *XPO1-MLLT10*$^+$ case was very similar to that in the *PICALM-MLLT10*$^+$ cases (Figure 1C). A targeted RT-PCR screen of 84 HOXA$^+$ T-ALL samples that lacked known explicatory genetic anomalies identified no further *XPO1-MLLT10*$^+$ cases (Figure 1D), suggesting rarity and/or breakpoint heterogeneity.

Each of the genes involved in this fusion has been previously implicated in leukemia. Notably, *MLLT10* (which encodes the AF10 protein) is involved in the recurrent *PICALM-MLLT10*[3] and *MLL-MLLT10*[4] translocations in both T-ALL and acute myeloblastic leukemia. Recently reported results of RNA-sequencing have identified *HNRNPH1* and *DDX3X* as *MLLT10* fusion partners in HOXA$^+$ T-ALL.[5] Our data provide further evidence of shared fusion partner–independent mechanisms of AF10-mediated transcriptional dysregulation, and this case adds to the repertoire of MLL and/or AF10-rearranged T-ALL that might be candidates for targeted DOT1L-directed therapy.[6] *MLLT10* breakpoints are heterogeneous, and increasing truncation of the transcript was reported to correlate with an earlier maturation block in T-ALL, although this was not confirmed in a later series.[3,7] In this case, detailed characterization of T-cell receptor (*TR*) gene configuration revealed monoallelic *TRG* and *TRD* and incomplete *TRB* diversity-joining rearrangements (data not shown), consistent with an immature pre-β-selection immunogenotype.[8]

XPO1 (also *CRM1*) encodes exportin 1, a transport protein that mediates nuclear export of multiple tumor suppressor and growth regulatory molecules (eg, P53 and RB1). Pharmacologic XPO1 inhibition has shown promising antileukemic activity in preclinical models via a mechanism that is believed to involve either nuclear retention of XPO1 cargo upon which the leukemic cells depend for survival,[9] and/or reactivation of nuclear protein phosphatase 2A.[10] It is tempting to speculate that HOXA-independent activity of the XPO1-AF10 fusion protein could also contribute to leukemogenesis in this case, for example through aberrant transport of proteins that mediate proliferation and survival and/or by dominant negative inhibition of wild-type XPO1.

Jonathan Bond
Université Sorbonne Paris Cité, Faculty of Medicine Descartes, INSERM U1151, Laboratory of Onco-Hematology, Assistance Publique-Hôpitaux de Paris, Hôpital Necker-Enfants Malades, Paris, France

Aurélie Bergon
Transcriptomic and Genomic Marseille-Luminy, Infrastructures en Biologie Santé et Agronomie Platform, Marseille, France
Technological Advances for Genomics and Clinics, INSERM U1090, Aix-Marseille University Unité Mixtes de Recherche-S 1090, Marseille, France

Amandine Durand
Université Sorbonne Paris Cité, Faculty of Medicine Descartes, INSERM U1151, Laboratory of Onco-Hematology, Assistance Publique-Hôpitaux de Paris, Hôpital Necker-Enfants Malades, Paris, France

Isabelle Tigaud
Cytogenetic and Molecular Biology Laboratory, Centre Hospitalier Lyon Sud, Pierre-Bénite, France

Xavier Thomas
Department of Hematology, Hôpital Edouard Herriot, Lyon, France

Vahid Asnafi
Université Sorbonne Paris Cité, Faculty of Medicine Descartes, INSERM U1151, Laboratory of Onco-Hematology, Assistance Publique-Hôpitaux de Paris, Hôpital Necker-Enfants Malades, Paris, France

Salvatore Spicuglia
Technological Advances for Genomics and Clinics, INSERM U1090, Aix-Marseille University Unité Mixtes de Recherche-S 1090, Marseille, France

Elizabeth Macintyre
Université Sorbonne Paris Cité, Faculty of Medicine Descartes, Institut Necker-Enfants Malades, INSERM U1151, Laboratory of Onco-Hematology, Assistance Publique-Hôpitaux de Paris, Hôpital Necker-Enfants Malades, Paris, France

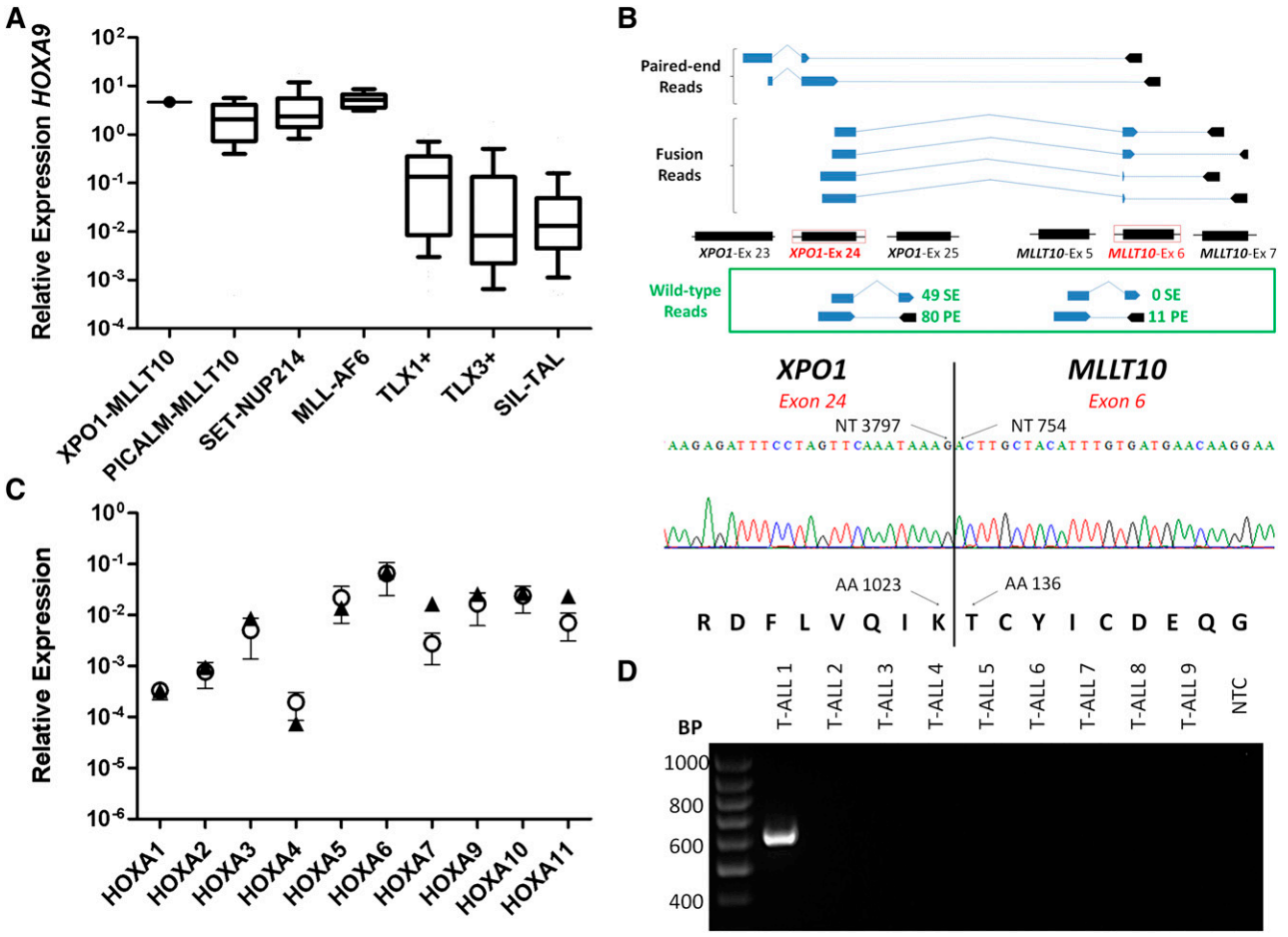

Figure 1. *XPO1-MLLT10* fusion detected by RNA-sequencing is associated with deregulation of *HOXA* gene locus expression. (A) Expression of *HOXA9* in genetic subgroups of T-ALL. Levels were determined by quantitative reverse transcriptase polymerase chain reaction (qRT-PCR) and calculated relative to an *ABL* housekeeping gene control. Boxes encompass the 25th through 75th percentiles, with the horizontal bar denoting the median expression level. Whiskers indicate the 10th and 90th percentiles. The numbers of cases tested in each group were as follows: *XPO1-MLLT10*, n = 1; *PICALM-MLLT10*, n = 36; *SET-NUP214*, n = 18; *MLL-AF6*, n = 9; *TLX1*$^{+}$, n = 86; *TLX3*$^{+}$, n = 67; *SIL-TAL*, n = 40. (B) Upper panel: Genomic mapping of the *XPO1-MLLT10* fusion by poly(A)-enriched strand-specific RNA-sequencing using the SOLiD HQ5500xl system (Life Technologies). Mapping, coverage, and fusion discovery were determined by using LifeScope (Life Technologies), with reference to version hg19 of the human genome. A schematic representation of paired-end and fusion-spanning reads that revealed fusion between exon 24 of *XPO1* (chr2:61708320-61708416) and exon 6 of *MLLT10* (chr10:21901277-21901380) is shown. Solid lines indicate split reads spanning 2 exons, and dotted lines indicate 2 reads of the same fragment. The numbers of unique reads for the wild-type *XPO1* (exons 24 and 25) and *MLLT10* (exons 5 and 6) transcripts are also depicted. Lower panel: Confirmation of expression of an in-frame *XPO1-MLLT10* fusion transcript by direct (Sanger) sequencing. The positions of the nucleotide (NT) and amino acid (AA) at the breakpoint of each gene are annotated. (C) Expression of *HOXA* genes in *XPO1-MLLT10*$^{+}$ (n = 1; denoted by triangles) and *PICALM-MLLT10*$^{+}$ (n = 4; mean levels denoted by circles with error bars indicating standard error of the mean) blasts. Transcript quantification was determined by qPCR using a TaqMan Low-Density Array, and the results of 2 experimental replicates were combined. Expression was calculated relative to a *GAPDH* housekeeping gene control. (D) RT-PCR for *XPO1-MLLT10*; 84 cases of HOXA^{+} T-ALL lacking known explicatory genetic anomalies were screened by using primers specific for the *XPO1-MLLT10* fusion transcript (product size, 618 bp). A representative PCR result is shown. T-ALL 1 is the index *XPO1-MLLT10*$^{+}$ case. NTC, no template control; PE, paired-end; SE, single-end.

Acknowledgments: This work was supported by a Kay Kendall Leukaemia Fund Intermediate Research Fellowship (J.B.), grants from INSERM, Groupement d'Intérêt Scientifique Infrastructures en Biologie Santé et Agronomie, Aix-Marseille Université, and grant No. ANR-10-INBS-0009-10 (for high throughput sequencing at the Transcriptomic and Genomic Marseille-Luminy Platform); a grant from the European Union's FP7 Program (agreement No. 282510-BLUEPRINT) (S.S.); the Association pour la Recherche sur le Cancer (project No. SFI20111203756), by the Aix-Marseille Initiative d'Excellence project (No. ANR-11-IDEX-0001-02); the Cancer Banking Network of the Institut National du Cancer (E.A.M.); the 2007 and 2012 (Caracteristique Moléculaire et Épigenetique des Leucémies Aiguës Myéloïdes de l'Enfant) Translational Research Programs in Immature T/Myeloid Acute Leukemias; and the Association Laurette Fugain.

Contribution: J.B., A.B., A.D., and I.T. performed research; X.T. performed patient management; J.B., A.B., V.A., S.S., and E.A.M. analyzed and interpreted data; and J.B., A.B., S.S., and E.M. wrote the manuscript.

Conflict-of-interest disclosure: The authors declare no competing financial interests.

Correspondence: Elizabeth A. Macintyre, Laboratoire Hématologie Biologique, Tour Pasteur 2ème étage, Hôpital Necker-Enfants Malades, 149 rue de Sèvres, 75743 Paris Cedex 15, France; e-mail: elizabeth.macintyre@nck.aphp.fr.

References

1. Soulier J, Clappier E, Cayuela JM, et al. HOXA genes are included in genetic and biologic networks defining human acute T-cell leukemia (T-ALL). *Blood.* 2005;106(1):274-286.
2. Van Vlierberghe P, van Grotel M, Tchinda J, et al. The recurrent SET-NUP214 fusion as a new HOXA activation mechanism in pediatric T-cell acute lymphoblastic leukemia. *Blood.* 2008;111(9):4668-4680.
3. Ben Abdelali R, Asnafi V, Petit A, et al. The prognosis of CALM-AF10-positive adult T-cell acute lymphoblastic leukemias depends on the stage of maturation arrest. *Haematologica.* 2013;98(11):1711-1717.
4. Meyer C, Hofmann J, Burmeister T, et al. The MLL recombinome of acute leukemias in 2013. *Leukemia.* 2013;27(11):2165-2176.
5. Brandimarte L, Pierini V, Di Giacomo D, et al. New MLLT10 gene recombinations in pediatric T-acute lymphoblastic leukemia. *Blood.* 2013;121(25):5064-5067.

6. Daigle SR, Olhava EJ, Therkelsen CA, et al. Potent inhibition of DOT1L as treatment of MLL-fusion leukemia. *Blood.* 2013;122(6): 1017-1025.

7. Asnafi V, Radford-Weiss I, Dastugue N, et al. CALM-AF10 is a common fusion transcript in T-ALL and is specific to the TCRgammadelta lineage. *Blood.* 2003; 102(3):1000-1006.

8. Asnafi V, Beldjord K, Boulanger E, et al. Analysis of TCR, pT alpha, and RAG-1 in T-acute lymphoblastic leukemias improves understanding of early human T-lymphoid lineage commitment. *Blood.* 2003;101(7):2693-2703.

9. Etchin J, Sanda T, Mansour MR, et al. KPT-330 inhibitor of CRM1 (XPO1)-mediated nuclear export has selective anti-leukaemic activity in preclinical models of T-cell acute lymphoblastic leukaemia and acute myeloid leukaemia. *Br J Haematol.* 2013;161(1):117-127.

10. Walker CJ, Oaks JJ, Santhanam R, et al. Preclinical and clinical efficacy of XPO1/CRM1 inhibition by the karyopherin inhibitor KPT-330 in Ph+ leukemias. *Blood.* 2013;122(17):3034-3044.

To the editor:

Two types of amyloid in a single heart

Amyloidosis is a heterogeneous group of diseases, in which amyloidogenic precursor proteins misfold and adopt a β-pleated sheet conformation.[1] Several proteins can form amyloid fibrils in vivo including transthyretin,[2] apolipoprotein A-I and A-II, lysozyme, fibrinogen, serum amyloid A protein and immunoglobulin light chains, but "cross-fibril" seeding appears to be rare such that 2 types of amyloid are rarely identified in the same individual.[3] Congo red (CR) staining with apple green birefringence under polarized light is used to confirm the presence of amyloid,[4] whereas immunohistochemistry, staining the biopsy tissue with a panel of monospecific antibodies against known amyloidogenic proteins, is the technique most widely used to characterize the amyloid fibril protein, but it is flawed.[5] Proteomic analysis involves proteolytic cleavage of proteins within microdissected amyloidotic tissue and identification by mass spectometry.[6] This additional tool is being increasingly used in conjunction with immunohistochemistry to identify the amyloid fibril protein.

We describe a case in which 2 amyloid fibril proteins were isolated in an individual patient both by immunohistochemistry and by proteomic analysis. An 81-year-old man was referred to our center with a 6- to 7-month history of exertional dyspnea and New York Heart Association class II symptoms. Baseline investigations included an echocardiogram showing characteristic features of cardiac amyloidosis with a thickened interventricular wall of 18 mm, moderate diastolic dysfunction, and preserved left ventricular ejection fraction of 58% accompanied by elevated serum cardiac biomarkers (*N*-terminal fragment brain natriuretic peptide 1966 ng/L and troponin T 0.09 μg/mL). ^{123}I-labeled serum amyloid P component scintigraphy did not show visceral amyloid deposits,[7] but ^{99m}Tc-dicarboxypropane diphosphonate (^{99m}Tc-DPD) scintigraphy showed abnormal (Perugini grade 2) cardiac uptake, typical of cardiac transthyretin amyloidosis[8] and unusual in light chain (AL) amyloidosis.[9] The κ-serum free light chain concentration was 13.1 mg/L, λ was 644 mg/L, and λ BJP was present. A bone marrow biopsy showed 6% plasma cells and immunophenotyping isolated a $CD19^-$, $CD56^+$, $CD27^+$ plasma cell clone. Sequencing of the transthyretin gene was wild-type. The differential diagnosis was between wild-type cardiac transthyretin (ATTR) amyloidosis (senile systemic amyloidosis) and cardiac AL amyloidosis, the management and prognosis of which differ substantially. A cardiac biopsy was undertaken to differentiate between these diagnoses. Figure 1 shows CR and immunohistochemical staining of the specimen using antibodies to λ light chains and transthyretin, and the results of proteomic analysis. Interestingly, there were 2 distinct patterns of amyloid within the same specimen: 1 showed honeycomb morphology, lighter CR staining, and stained with antibody against transthyretin, but not λ light chains, and the other showed more diffuse, but darker CR staining, and stained with antibody against λ light chains, but not transthyretin. The 2 distinct areas were separately captured by laser microdissection and analyzed by tandem mass spectrometry. Amyloid was identified by its "signature proteins" in both samples, but in 1 there was abundant transthyretin with low level λ light chain and in the other there was abundant λ light chain without transthyretin (Figure 1D), thus confirming the immunohistochemistry results of 2 types of amyloid in the same heart. Our patient is due to receive chemotherapy for AL amyloidosis shortly.

In summary, the exceptionally rare occurrence of 2 different amyloid fibril proteins was suggested by immunohistochemistry in this patient. The coexistence of 2 amyloid types in the same heart was confirmed by laser capture microdissection and proteomic analysis of 2 distinct areas.

Shameem Mahmood
National Amyloidosis Centre, University College London Medical School, Royal Free Hospital Campus, London, United Kingdom

Janet A. Gilbertson
National Amyloidosis Centre, University College London Medical School, Royal Free Hospital Campus, London, United Kingdom

Nigel Rendell
National Amyloidosis Centre, University College London Medical School, Royal Free Hospital Campus, London, United Kingdom

Carol J. Whelan
National Amyloidosis Centre, University College London Medical School, Royal Free Hospital Campus, London, United Kingdom

Helen J. Lachmann
National Amyloidosis Centre, University College London Medical School, Royal Free Hospital Campus, London, United Kingdom

Ashutosh D. Wechalekar
National Amyloidosis Centre, University College London Medical School, Royal Free Hospital Campus, London, United Kingdom

Philip N. Hawkins
National Amyloidosis Centre, University College London Medical School, Royal Free Hospital Campus, London, United Kingdom

Julian D. Gillmore
National Amyloidosis Centre, University College London Medical School, Royal Free Hospital Campus, London, United Kingdom